Journal of the Korean Chemical Society
2005, *Vol. 49, No. 1*
Printed in the Republic of Korea

N-Pentane의 평형 구조에 대한 진동 분광학 연구

Liangyu Wang* and Yunhong Zhang
베이징공과대학 화학과
(2004. 11. 8 접수)

Vibrational Study of the Chain Conformation of the n-pentane

Liangyu Wang* and Yunhong Zhang
Department of Chemistry, Beijing Institute of Technology, Beijing, China 100081
(Received November 8, 2004)

요 약. *n*-Pentane의 세가지 평형 구조에 대한 진동 스펙트럼을 예측하기 위하여 순이론 계산을 수행하였다. *n*-Pentane의 분자 구조와 진동 스펙트럼의 상관 관계를 규명하기 위하여 실험적으로 측정한 IR, Raman 스펙트럼과 계산된 결과들을 비교, 분석하였다. 그 결과, 실험으로 관측된 진동 밴드들과 이론적으로 계산된 값들은 잘 일치되었으며, 특성적인 평형 구조에 대한 서로 다른 진동 밴드들 또한 명확하게 해석될 수 있었다. 각 평형 구조에 따른 진동 밴드의 변화 경향성이 논의되었다.

주제어: 순이론계산, 진동분광학, 평형 구조, 펜탄

ABSTRACT. *Ab initio* calculations were used to calculate normal mode frequencies and intensities of three stable conformations of n-pentane. The overall frequency region including IR and Raman spectra were analyzed to get the full spectra of n-pentane and to explore the relations between frequency and disorder in the overall frequency region. The bands in the IR spectra and in the Raman spectra were found to be associated with specific conformations, and therefore the characteristic bands of each conformation could be obtained. For the bands with the same vibrational modes, the trend with the change of conformation was also discussed.

Keywords: *Ab initio*, Vibrational Spectroscopy, Conformation, *n*-Pentane

INTRODUCTION

Vibrational spectroscopy has been used extensively to identify and characterize rotational isomeric structures of n-alkanes, e.g., providing information on quantities such as configuration, conformation, chemical composition and orientation. A major contribution to the analysis of vibrational spectra, particularly in the conformational dependence of alkanes and polyethylene, was presented by Snyder and Schachtschneider with the empirically refined force fields.[1-3] But such force fields could not provide detailed insights into the conformation dependence of force constants and spectra, it was therefore important to have complete understanding of those properties that could be obtained by *ab initio* calculations.[4-7] With the current *ab initio* calculations, it would become possible to calculate vibrational frequencies and the corresponding intensities especially for the small molecules. Hence, small alkanes of trans (*t*) and gauche (*g*) conformations had been studied widely since their structure and bonding served as protypes for carbon-based chemical industry. *Ab initio* vibrational frequencies and optimized geometry research had been conducted on propane[8-10] at different levels of theory and the n-butane molecule also commanded obvious interest and had been studied extensively by theoretical methods.[11-18] How-

ever, for longer n-alkanes, their stable conformers provided combinations of *t* and *g* rotational states that were available in n-butane, it was important to extend these studies. *Ab initio* methods also used to calculate pentane and hexane conformations with the basis sets of HF/4-21G,[17,18] HF/4-31G[4] and HF/6-31G,[14,19] which provided spectra studies of four stable conformers of n-pentane and 10 stable conformers of n-hexane and the insights of the influence of conformation on these other molecular properties. In addition, Synder and Kim[20] had studied Raman spectra of liquid n-alkanes C_4-C_9 and presented the overall Raman intensity in the low frequency range. Meanwhile, a wide range of experimental techniques, such as NMR,[21-23] IR[24-26] and Raman,[27] had been employed to reveal the molecular features of the n-alkyl chains. However, the studies mentioned above only gave the amount of conformational disorder at a specific site in the *n*-alkyl chains. Due to the limitation of experimental conditions, it is very difficult to get the overall frequency information of the conformational order of these systems by experiments. Hence *ab initio* calculations were of importance to solve this problem. At the same time, as a basic unit, it could provide some useful information of the conformation for long chain n-alkanes by analyzing the results of *n*-pentane. Therefore we could use *n*-pentane as a model for long chain *n*-alkanes, even though there were many more complex conformations. The *n*-pentane undertook four conformations of the carbon backbone. With respect to the current study, the presence of three stable conformations of *n*-pentane meant that the spectra could be interpreted as resulting from three spectroscopically different species, each having its own set of vibrational frequency and intensity parameters. According to the IR and Raman frequencies and intensities of each conformation, the detailed spectra information of the specific conformation and the corresponding correlation between frequency and vibrational mode could be obtained. Hence, *ab initio* calculations were useful tools to carry out the vibrational study of *n*-alkanes.

CALCULATIONS

Ab initio calculations were performed with the GAUSSIAN 98[28] programs. The Hartree-Fock (HF) method and the 6-31G basis set were used to obtain the optimized geometries and frequencies for each molecule in this work. For the n-alkanes, the 6-31G basis set[19, 29] was proved to be good enough. The internal and local symmetry coordinates for each molecule followed the definitions of the *tt* conformation of n-pentane (see *Fig.* 1), both *gt* and *gg* conformations were just the same as the above description (see *Fig.* 2 and *Fig.* 3). The optimized geometries of all the *n*-pentane conformations at

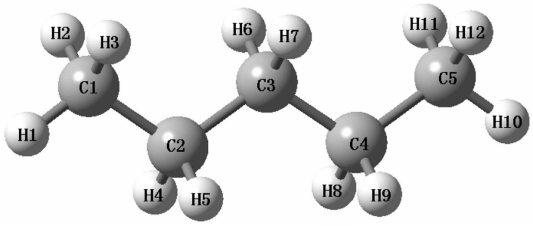

Fig. 1. Internal coordinates of *tt* conformation of *n*-pentane.

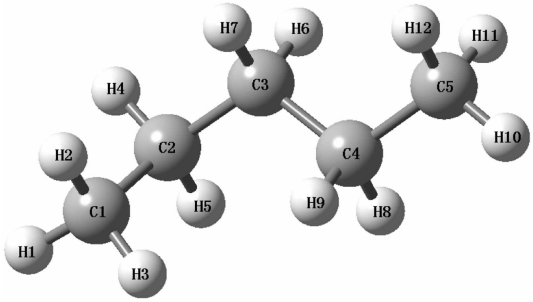

Fig. 2. Internal coordinates of *gt* conformation of *n*-pentane.

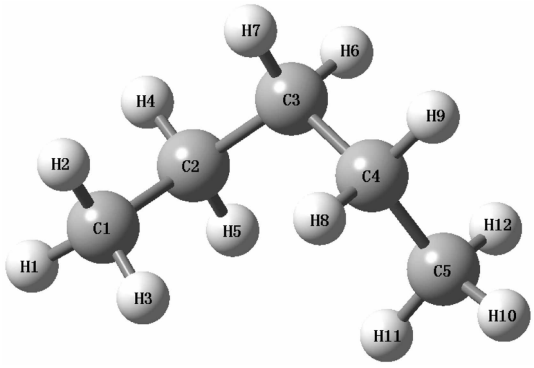

Fig. 3. Internal coordinates of *gg* conformation of *n*-pentane.

Table 1. Optimized geometries of conformers of *n*-pentane with 6-31G basis set

coordinate	*tt*	*gt*	*gg*	coordinate	*tt*	*gt*	*gg*
C1C2	1.531	1.533	1.532	C3C2H4	109.3	108.6	108.1
C2C3	1.533	1.536	1.537	C3C2H5	109.3	109.2	110.0
C3C4	1.533	1.534	1.537	C4C3H6	109.2	108.6	108.6
C4C5	1.531	1.532	1.532	C4C3H7	109.2	109.2	108.6
C1H1	1.085	1.085	1.085	C3C4H8	109.4	109.1	110.0
C1H2	1.085	1.086	1.086	C3C4H9	109.4	110.0	108.1
C1H3	1.085	1.084	1.084	C4C5H10	111.3	111.3	110.9
C2H4	1.087	1.087	1.087	C4C5H11	111.1	111.1	111.9
C2H5	1.087	1.088	1.086	C4C5H12	111.1	111.0	111.0
C3H6	1.088	1.088	1.088	C1C2C3C4	180.0	66.5	62.3
C3H7	1.088	1.088	1.088	C2C3C4C5	180.0	176.6	62.3
C4H8	1.087	1.088	1.087	C3C2C1H1	180.0	175.9	175.0
C4H9	1.087	1.086	1.086	C3C2C1H2	59.9	56.3	55.3
C5H10	1.085	1.085	1.085	C3C2C1H3	-59.9	-64.1	-65.1
C5H11	1.085	1.085	1.084	C4C3C2H4	-58.0	-171.9	-176.5
C5H12	1.085	1.085	1.086	C4C3C2H5	58.0	-56.4	-61.3
C1C2C3	113.0	114.3	114.2	C5C4C3H6	58.0	54.9	-60.2
C2C3C4	113.3	114.5	115.8	C5C4C3H7	-58.0	-60.6	-175.3
C3C4C5	113.0	112.6	114.2	C2C3C4H8	58.0	54.9	-61.3
C2C1H1	111.3	110.9	110.9	C2C3C4H9	-58.0	-61.5	-176.5
C2C1H2	111.1	110.9	111.0	C3C4C5H10	180.0	179.9	175.0
C2C1H3	111.1	111.9	111.9	C3C4C5H11	-59.9	-60.0	-65.1
				C3C4C5H12	59.9	60.0	55.3

*Bond lengths in angstroms, bond angles in degrees.

this level of theory were shown in *Table* 1. In general, the HF *ab intio* calculated frequencies were higher than the corresponding experimental values due to neglect of contributions from electron correlation. In this work, the calculated and observed frequencies were not compared and no scaling of vibrational frequencies was applied. But the relations between the calculated frequencies and the conformations and the trend of frequency changes were discussed in detail.

RESULTS AND DISCUSSIONS

The calculated frequencies of the following molecules were used in the refinement: *tt*, *gt* and *gg* for *n*-pentane. The *gg'* form was the least stable[19] because of the steric hindrance, and therefore the *gg'* conformation was not discussed in this paper. With respect to the optimized geometries of all pentane conformations, the CH bond lengths and the CCH bond angles were the least affected by conformation. On the other hand, the internal CC bond lengths and CCC angles were the most affected by conformational changes, there being a tendency for those to be larger than the terminal ones. The *tt* conformation had C_{2v} symmetry, while the gg conformation had C_2 symmetry. And for *gt* conformation of *n*-pentane, it had lower symmetry. Hence the vibrations associated with an assembly of conformational disordered chains were much more difficult to characterize. But they all had 45 fundamental frequencies including vibrational modes with IR and Raman active, those only with IR active or only with Raman active.

The low frequency region (0-600 cm^{-1}) of the IR and Raman spectra was useful for analyzing polymethylene chain conformation. There remained some problems, however, concerning the interpretation of the spectra obtained by experiments. Hence the present analysis of calculated spectra of n-pentane

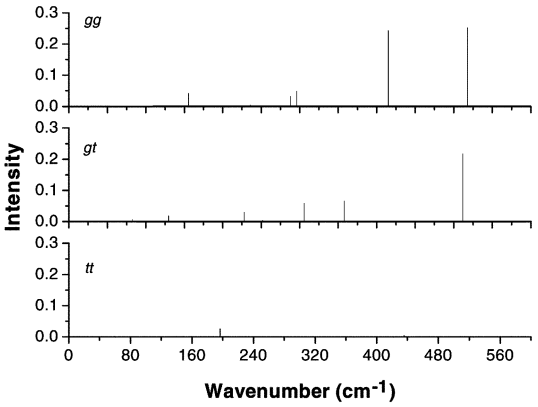

Fig. 4. Calculated IR spectra of *n*-pentane in the region of 0-600 cm^{-1}.

was aimed at improving band assignments and exploring the relations between frequency and conformation in this region. With the changes of the conformation, the vibrational modes would become more complex. In order to characterize the vibrations of an assembly of disordered chains in detail, the coordinates are defined as follows: s is stretching; ss is symmetric stretching; as is antisymmetric stretching; b is bending; sb is symmetric bending; ab is antisymmetric bending; r is rocking; w is wagging; tw is twisting; t is torsion. The calculated IR spectra (0-600 cm^{-1}) were shown in *Fig.* 4 and the assignments of main bands were listed in *Table* 2. It was obvious that there were great differences between *tt* conformation and *gt* or *gg* conformation. For all-trans conformation there was only a single band, at 196.4 cm^{-1}, with appreciable intensity in the calculated IR spectra of n-pentane, whereas for *gt* conformation there were four bands with appreciable intensity, the band with the highest intensity was at 511.7 cm^{-1}. The *gg* conformation had five bands with higher intensity. Different from *gt* conformation, the intensities of the bands of 414.9 cm^{-1} and 517.9 cm^{-1} were relatively higher. Especially interesting was that the vibrational modes mentioned above belonged to CCC bending mode, another kind of mode, at 305.6 cm^{-1} (*gt*), 296.5 cm^{-1} and 155.3 cm^{-1} (*gg*), belonged to CC torsion mode or methyl torsion mode. The proposed assignments,[30] obtained by high resolution neutron scattering, to CCC bending mode were at 401 cm^{-1} and 190 cm^{-1}. And the earlier force fields[3] predicted that the methyl torsion modes were at 215 and 210 cm^{-1}. Tomonaga[31] measured the far infrared spectra of *n*-pentane and found that bands at 470 and 334 cm^{-1} were assignable to the *gt* conformation and a band at 386 cm^{-1} assignable to the *gg* conformation. The frequencies mentioned above were well in agreement with our calculated values, even though some of our assignments to conformations differed from those previously proposed.[3] From the calculated results, we could find some bands that mainly occurred at the fold site of *gt* or *gg* conformation, thus these bands could be regarded as the characteristic bands. In this region, there was only one characteristic band: 511.7 cm^{-1} for *gt* conformation, 517.9 cm^{-1} for *gg* conformation respectively. But for *tt* conformation, the bands with higher intensity were considered as its characteristic bands, thus the band at 196.4 cm^{-1} was the characteristic band of *tt* conformation. As far as the effect of changes in

Table 2. Calculated IR frequency and description of 0-600 cm^{-1}

Conformation	Calculated frequency (cm^{-1})	Description
tt	196.4	$b(C_{2,3,4})$
gt	227.6	$t(C_1H_{12,3}), b(C_{2,3,4})$
	305.6	$t(C_1H_{12,3}), t(C_{12}C_{2,3})$
	358.1	$b(C_{12,3}C_{2,3,4}C_{3,4,5})$
	511.7	$b(C_{12,3}, C_{3,4,5}).b(C_{2,3,4})$
gg	155.3	$t(C_1H_{12,3}), t(C_3H_{(5+6),(7+8)})$
	287.8	$b(C_{12,3}C_{2,3,4}C_{3,4,5})$
	296.5	$t(C_1H_{12,3}), t(C_{12}C_{2,3}),t(C_3H_{(5+6),(7+8)}), t(C_{3,4}C_{4,5})$
	414.9	$b(C_{12,3}),b(C_{3,4,5})$
	517.9	$b(C_{12,3}, C_{3,4,5}).b(C_{2,3,4})$

conformation was concerned, the change trend of the same vibrational modes was only discussed. For the vibrational mode of $b(C_{1,2,3},C_{2,3,4},C_{3,4,5})$ (stand for in-phase CCC bending), with the change of conformation from *tt* to *gt* and *gg*, the frequency decreased from 428.6 cm^{-1}, 358.1 cm^{-1} to 287.8 cm^{-1}. But the intensities of *gt* and *gg* conformations were stronger than that of *tt* conformation. For the vibrational mode of $b(C_{1,2,3}, C_{3,4,5})b(C_{2,3,4})$ (stand for out-of-phase CCC bending), the frequency increased from 511.7 to 517.9 cm^{-1} with the conformation changed from *gt* to *gg*.

The calculated Raman spectra (0-600 cm^{-1}) were shown in *Fig.* 5 and the descriptions of main bands were listed in *Table* 3. Compared with the calculated IR spectra, although the intensities of the main bands were higher than those of IR, the number of the bands with higher intensity was fewer than that of IR and the mode of vibration was only CCC bending. At the same time, there were significant differences between the bands of *tt* and *gt*, *gg* conformations. For all-trans conformation there was only a single band at 428.6 cm^{-1}, with the highest intensity ,whereas for *gt* and *gg* conformation there were two main bands respectively, 511.7 and 358.1 cm^{-1} with middle intensities for *gt* conformation, 517.9 and 287.8 cm^{-1} with weak intensities for *gg* conformation. Snyder and Kim[20] presented the calculated Isotropic Raman spectra of n-pentane in the low frequency (0-600 cm^{-1}) and suggested that the band at 400 cm^{-1} should belong to *tt* conformation, the bands at 340 cm^{-1} and 470 cm^{-1} should belong to *gt* conformation. Those were consistent with our calculated values. But the bands of *gg* conformation had not been mentioned. From our calculated results, although the intensities of bands of *gg* conformation were much weaker, the bands at 517.9 cm^{-1} and 287.8 cm^{-1} should belong to *gg* conformation. In addition, there were the same characteristic bands with those in the IR spectra, 511.7 cm^{-1} for *gt* conformation, 517.9 cm^{-1} for *gg* conformation. However the characteristic band of *tt* conformation was at 428.6 cm^{-1}. Likewise, for the vibrational mode of $b(C_{1,2,3},C_{2,3,4},C_{3,4,5})$, the trend of frequency change with the conformation was the same as that in the IR spectra mentioned above.

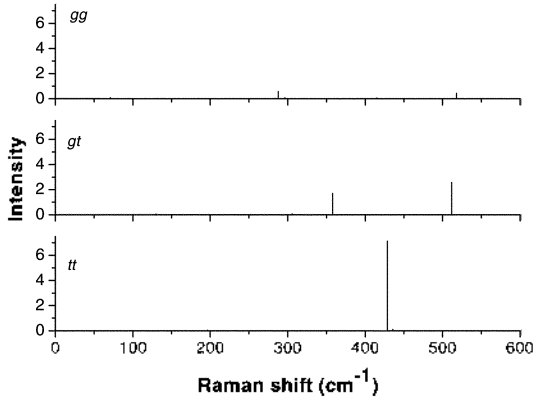

Fig. 5. Calculated Raman spectra of *n*-pentane in the region of 0-600 cm^{-1}.

Table 3. Calculated Raman frequency and description of 0-600 cm^{-1}

Conformation	Calculated frequency (cm^{-1})	Description
tt	428.6	$b(C_{1,2,3},C_{2,3,4},C_{3,4,5})$
gt	358.1	$b(C_{1,2,3},C_{2,3,4},C_{3,4,5})$
	511.7	$b(C_{1,2,3},C_{3,4,5})b(C_{2,3,4})$
gg	287.8	$b(C_{1,2,3},C_{2,3,4},C_{3,4,5})$
	517.9	$b(C_{1,2,3},C_{3,4,5})b(C_{2,3,4})$

Due to the intermolecular interactions, many vibrations had coupling in some degree. Thus the number and complexity of the bands in the region of 700-1300 cm^{-1} increased, especially for the *gt* conformation with lower symmetry. Hence the approximate nature of the vibrational modes was only described in this paper. The calculated IR spectra were shown in *Fig.* 6 and the assignments of main bands were listed in *Table* 4. Early study had reported[3] that there were two bands whose vibrational mode was methylene rocking (in-phase) for *n*-pentane, the band at 733 cm^{-1} with higher intensity belonged to *gt* conformation and the band at 728 cm^{-1} with lower intensity belonged to *tt* conformation. And this result was consistent with our calculated values, for *tt* conformation at 803.4 cm^{-1}, for *gt* conformation at 811.9 cm^{-1} and for gg conformation at 807.2 cm^{-1}. Based on the rule of characteristic bands mentioned above, the characteristic bands of each conformation were as follows: 803.4 cm^{-1},

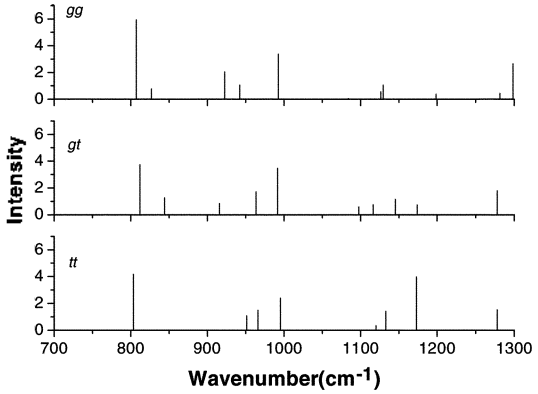

Fig. 6. Calculated IR spectra of *n*-pentane in the region of 700-1300 cm^{-1}.

995.4 cm^{-1} and 1172.7 cm^{-1} for *tt* conformation; 844.2 cm^{-1}, 915.8 cm^{-1} and 1174.1 cm^{-1} for *gt* conformation; 807.2 cm^{-1} and 922.6 cm^{-1} for *gg* conformation in this region. On the other hand, there were other two important vibrational modes: CC stretching mode and methyl rocking mode. And both of the bands often appeared at the same time. For the vibrational mode r($C_1H_{1,2,3}$,$C_5H_{10,11,12}$)s($C_{1,2}$,$C_{2,3}$)s($C_{3,4}$,$C_{4,5}$), when the conformation changed from *tt* to *gt* and *gg*, the calculated frequency would shift about 4 cm^{-1} at most, 995.4 cm^{-1} for *tt* conformation, 991.8 cm^{-1} for *gt* conformation and 992.8 cm^{-1} for *gg* conformation. Another apparent character was at near 1300 cm^{-1}, the r($C_1H_{1,2,3}$,$C_5H_{10,11,12}$)s($C_{1,2}$,$C_{2,3}$,$C_{3,4}$,$C_{4,5}$) vibrational mode also varied, 1278.0 cm^{-1} for *tt* conformation, 1278.1 cm^{-1} for *gt* conformation and 1281.2 cm^{-1} for *gg* conformation. However, the intensity of *gg* conformation was so weak that it was not listed in the *Table* 4.

The calculated Raman spectra (700-1300 cm^{-1}) were shown in *Fig.* 7 and the assignments of main bands were listed in *Table* 5. Compared with the calculated IR spectra, there was a great difference between the spectra of *tt* conformation and the *gt*, *gg* conformation. For the vibrational mode of r($C_1H_{1,2,3}$,

Table 4. Calculated IR frequency and description of 700-1300 cm^{-1}

Conformation	Calculated frequency (cm^{-1})	Description
tt	803.4	r($C_2H_{4,5}$,$C_3H_{6,7}$,$C_4H_{8,9}$)
	951.4	s($C_{2,3}$,$C_{3,4}$), r($C_1H_{1,2,3}$,$C_5H_{10,11,12}$)
	965.9	r($C_3H_{6,7}$),r($C_1H_{2,3}$,$C_2H_{4,5}$,$C_4H_{8,9}$,$C_5H_{11,12}$)
	995.4	r($C_1H_{1,2,3}$,$C_5H_{10,11,12}$),s($C_{1,2}$,$C_{2,3}$),s($C_{3,4}$,$C_{4,5}$)
	1132.8	s($C_{1,2}$,$C_{3,4}$),s($C_{2,3}$,$C_{4,5}$),r($C_1H_{1,2,3}$,$C_5H_{10,11,12}$),w($C_3H_{6,7}$)
	1172.7	s($C_{2,3}$,$C_{3,4}$) ,w($C_2H_{4,5}$,$C_4H_{8,9}$),r($C_1H_{1,2,3}$,$C_5H_{10,11,12}$)
	1278.0	s($C_{1,2}$,$C_{2,3}$,$C_{3,4}$,$C_{4,5}$),r($C_1H_{1,2,3}$,$C_5H_{10,11,12}$)
gt	811.9	r($C_2H_{4,5}$,$C_3H_{6,7}$,$C_4H_{8,9}$)
	844.2	s($C_{1,2}$,$C_{2,3}$,$C_{3,4}$,$C_{4,5}$),r($C_2H_{4,5}$,$C_4H_{8,9}$)
	915.8	r($C_1H_{1,2,3}$,$C_5H_{10,11,12}$),s($C_{2,3}$,$C_{3,4}$)
	963.3	r($C_1H_{1,2,3}$,$C_5H_{10,11,12}$),tw($C_2H_{4,5}$,$C_4H_{8,9}$)
	991.8	r($C_1H_{1,2,3}$,$C_5H_{10,11,12}$),s($C_{1,2}$,$C_{2,3}$),s($C_{3,4}$,$C_{4,5}$)
	1097.5	s($C_{1,2}$,$C_{4,5}$),s($C_{2,3}$,$C_{3,4}$),r($C_1H_{1,2,3}$,$C_5H_{10,11,12}$),tw($C_3H_{6,7}$)
	1116.3	r($C_1H_{1,2,3}$,$C_5H_{10,11,12}$),s($C_{3,4}$),s($C_{4,5}$),tw($C_3H_{6,7}$,$C_4H_{8,9}$)
	1145.5	r($C_1H_{1,2,3}$,$C_5H_{10,11,12}$),r($C_3H_{6,7}$,$C_4H_{8,9}$),tw($C_2H_{4,5}$)
	1174.1	s($C_{1,2}$,$C_{3,4}$),s($C_{2,3}$,$C_{4,5}$),r($C_2H_{4,5}$,$C_4H_{8,9}$),r($C_3H_{6,7}$)
	1278.1	r($C_1H_{1,2,3}$,$C_5H_{10,11,12}$),s($C_{1,2}$,$C_{2,3}$,$C_{3,4}$,$C_{4,5}$)
gg	807.2	r($C_2H_{4,5}$,$C_3H_{6,7}$,$C_4H_{8,9}$)
	827.1	s($C_{1,2}$,$C_{2,3}$,$C_{3,4}$,$C_{4,5}$)
	922.6	r($C_1H_{1,2,3}$,$C_5H_{10,11,12}$),s($C_{2,3}$,$C_{3,4}$)
	942.2	s($C_{1,2}$,$C_{2,3}$),s($C_{3,4}$,$C_{4,5}$)
	992.8	s($C_{1,2}$,$C_{2,3}$),s($C_{3,4}$,$C_{4,5}$),r($C_1H_{1,2,3}$,$C_5H_{10,11,12}$),r($C_3H_{6,7}$)
	1129.5	r($C_1H_{1,2,3}$),r($C_5H_{10,11,12}$),w($C_2H_{4,5}$),w($C_4H_{8,9}$),tw($C_3H_{6,7}$)
	1298.5	b($C_{1,2,3}$),b($C_{3,4,5}$),r($C_1H_{2,3}$,$C_5H_{10,11,12}$),r($C_3H_{6,7}$)

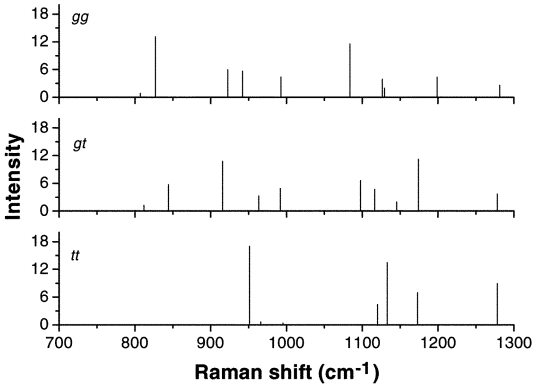

Fig. 7. Calculated Raman spectra of *n*-pentane in the region of 700-1300 cm $^{-1}$.

$C_5H_{(6,11,12)}$).s($C_{2,3}$,$C_{3,4}$), the band at 951.4 cm^{-1} was sharp for *tt* conformation, but the bands were broad for *gt* conformation at 915.8 cm $^{-1}$ and for *gg* conformation at 922.6 cm $^{-1}$. In the meanwhile, the intensity decreased gradually. Similarly, the vibrational mode of s($C_{1,2}$,$C_{2,3}$,$C_{3,4}$,$C_{4,5}$)r($C_1H_{1,2,3}$,$C_5H_{(10,11,12)}$), *tt* at 1278.0 cm $^{-1}$, *gt* at 1278.1 cm $^{-1}$ and *gg* at 1281.3 cm $^{-1}$, altered in the same way. With respect to the characteristic bands of each conformation, the bands for *tt* conformation were at 951.4 cm^{-1}, 1132.8 cm^{-1} and 1278.0 cm^{-1}: for *gt* conformation at 844.2 cm^{-1}, 915.8 cm^{-1} and 1174.1 cm $^{-1}$; for *gg* conformation at 922.6 cm $^{-1}$, 1083.8 cm $^{-1}$ and 1126.2 cm $^{-1}$ in this region.

The calculated IR spectra in the range of 1300-1700 cm $^{-1}$ were shown in *Fig.* 8 and the descriptions of main bands were listed in *Table* 6. In general, the bands were much better defined than those in the region of 700-1300 cm^{-1}, the vibrational modes mainly included the methylene wagging and bending, the methyl symmetric and antisymmetric bending. From *Fig.* 8, we could find that the intensities of the bands in the lower-frequency region were distinctly weaker than those in the higher-frequency region. Hence emphasis was put on the higher-frequency. The band at 1540.6 cm $^{-1}$ of *tt* conformation was the coupling between methylene wagging mode and CC stretching mode, the same vibrational mode was found at 1523.8 cm $^{-1}$ for *gt* conformation and at 1538.9 cm $^{-1}$ for *gg* conformation respectively. In addition, the shoulders at about

Table 5. Calculated Raman frequency and description of 700-1300 cm $^{-1}$

Conformation	Calculated frequency (cm^{-1})	Description
tt	951.4	r($C_1H_{1,2,3}$,$C_5H_{(10,11,12)}$).s($C_{2,3}$,$C_{3,4}$)
	1120.0	s($C_{1,2}$,$C_{4,5}$).s($C_{2,3}$,$C_{3,4}$)
	1132.8	s($C_{1,2}$,$C_{3,4}$).s($C_{2,3}$,$C_{4,5}$).r($C_1H_{1,2,3}$,$C_5H_{(6,11,12)}$).w($C_5H_{6,7}$)
	1172.7	s($C_{2,3}$,$C_{3,4}$) .w($C_2H_{4,5}$,$C_4H_{8,9}$).r($C_1H_{1,2,3}$,$C_5H_{(6,11,12)}$)
	1278.0	s($C_{1,2}$,$C_{2,3}$,$C_{3,4}$,$C_{4,5}$).r($C_1H_{1,2,3}$,$C_5H_{(10,11,12)}$)
gt	844.2	s($C_{1,2}$,$C_{2,3}$,$C_{3,4}$,$C_{4,5}$).r($C_2H_{4,5}$,$C_4H_{8,9}$)
	915.8	r($C_1H_{1,2,3}$,$C_5H_{(10,11,12)}$).s($C_{2,3}$,$C_{3,4}$)
	963.3	r($C_1H_{1,2,3}$,$C_5H_{(10,11,12)}$).tw($C_2H_{4,5}$,$C_4H_{8,9}$)
	991.8	r($C_1H_{1,2,3}$,$C_5H_{(10,11,12)}$).s($C_{1,2}$,$C_{2,3}$).s($C_{3,4}$,$C_{4,5}$)
	1097.5	s($C_{1,2}$,$C_{4,5}$).s($C_{2,3}$,$C_{3,4}$).r($C_1H_{1,2,3}$,$C_5H_{(6,11,12)}$).tw($C_5H_{6,7}$)
	1116.3	r($C_1H_{1,2,3}$,$C_5H_{(10,11,12)}$).s($C_{3,4}$).s($C_{4,5}$).tw($C_5H_{6,7}$,$C_4H_{8,9}$)
	1174.1	s($C_{1,2}$,$C_{3,4}$).s($C_{2,3}$,$C_{4,5}$).r($C_2H_{4,5}$,$C_4H_{8,9}$).r($C_5H_{6,7}$)
	1278.1	r($C_1H_{1,2,3}$,$C_5H_{(10,11,12)}$).s($C_{1,2}$,$C_{2,3}$,$C_{3,4}$,$C_{4,5}$)
gg	827.1	s($C_{1,2}$,$C_{2,3}$,$C_{3,4}$,$C_{4,5}$)
	922.6	r($C_1H_{1,2,3}$,$C_5H_{(10,11,12)}$).s($C_{2,3}$,$C_{3,4}$)
	942.2	s($C_{1,2}$,$C_{3,4}$).s($C_{3,4}$,$C_{4,5}$)
	992.8	s($C_{1,2}$,$C_{3,4}$).s($C_{3,4}$,$C_{4,5}$).r($C_1H_{1,2,3}$,$C_5H_{(6,11,12)}$).r($C_5H_{6,7}$)
	1083.8	s($C_{1,2}$,$C_{4,5}$).s($C_{2,3}$,$C_{3,4}$).tw($C_5H_{6,7}$)
	1126.2	s($C_{1,2}$,$C_{3,4}$).s($C_{2,3}$,$C_{4,5}$).w($C_5H_{6,7}$). r($C_1H_{1,2,3}$,$C_5H_{(6,11,12)}$).tw($C_2H_{4,5}$,$C_4H_{8,9}$)
	1198.5	s($C_{1,2}$,$C_{3,4}$).s($C_{2,3}$,$C_{4,5}$).w($C_2H_{4,5}$,$C_4H_{8,9}$),w($C_5H_{6,7}$)
	1281.3	r($C_1H_{1,2,3}$,$C_5H_{(10,11,12)}$).s($C_{1,2}$,$C_{2,3}$,$C_{3,4}$,$C_{4,5}$)

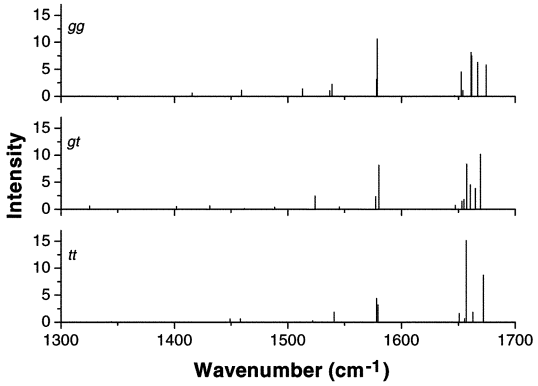

Fig. 8. Calculated IR spectra of *n*-pentane in the region of 1300-1700 cm^{-1}.

1578 cm^{-1} belonged to in-phase and out-of-phase methyl symmetric bending. According to the calculated results, the frequency of this mode was independent of conformation, e.g., for in-phase methyl symmetric bending, *tt* at 1578.1 cm^{-1}, *gt* at 1577.3 cm^{-1} and *gg* at 1578.3 cm^{-1}. The mode of out-of-phase symmetric bending had the same character. In the higher-frequency region, the vibrational mode was the coupling between methyl antisymmetric bending and methylene bending. With the decrease of symmetry, the coupling would become more serious because of the great effect of conformation. For *tt* conformation, there were two sharp bands, at 1656.9 cm^{-1} and 1672.0 cm^{-1} respectively, but it was almost impossible for *gt* and *gg* conformation. At the same time, the same vibrational mode was very difficult to find, therefore this was not discussed in this paper. With respect to the characteristic bands of each conformation, the characteristic bands of *tt* conformation were at 1656.9 cm^{-1} and 1672.0 cm^{-1}; for *gt* conformation at 1523.8 cm^{-1} and 1660.5 cm^{-1}; for *gg* conformation at 1652.5 cm^{-1}, 1667.0 cm^{-1} and 1674.3 cm^{-1} in this region.

From the calculated Raman spectra in the range of 1300-1700 cm^{-1} (shown in *Fig.* 9) and the assignments of main bands (listed in *Table* 7), we could see that the bands with higher intensity were mostly located at two sites: one at about 1461 cm^{-1}, the other at about 1660 cm^{-1}. For the former, the methylene twisting mode played an important role. For the latter, however, it comprised of three kinds of

Table 6. Calculated IR frequency and description of 1300-1700 cm^{-1}

Conformation	Calculated frequency (cm^{-1})	Description
tt	1540.6	$w(C_2H_{11},C_3H_{8,9},C_1H_{6,7}),s(C_{1,2},C_{3,4}),s(C_{2,5},C_{1,5})$
	1578.1	$sb(C_1H_{2,3},C_5H_{10,11,12})$
	1579.4	$sb(C_1H_{2,3}),sb(C_5H_{10,11,12})$
	1656.9	$ab(C_1H_{2,3},C_5H_{10,11,12})$
	1672.0	$b(C_1H_{2,3},C_2H_{11},C_3H_{8,9},C_1H_{6,7},C_5H_{11,12})$
gt	1523.8	$w(C_2H_{11},C_3H_{8,9},C_1H_{6,7}),s(C_{1,2},C_{3,4}),s(C_{2,5},C_{1,5})$
	1577.3	$sb(C_1H_{2,3},C_5H_{10,11,12})$
	1580.1	$sb(C_1H_{2,3}),sb(C_5H_{10,11,12})$
	1657.2	$ab(C_5H_{10,11,12})$
	1660.5	$b(C_1H_{2,3}),b(C_2H_{11},C_3H_{8,9})$
	1664.9	$b(C_2H_{11},C_3H_{8,9},C_5H_{11,12}),ab(C_1H_{12,5}),b(C_1H_{6,7})$
	1669.3	$ab(C_1H_{2,3}),ab(C_5H_{10,11,12}),b(C_2H_{11},C_3H_{8,9}),b(C_5H_{11,12})$
gg	1538.9	$w(C_2H_{11},C_3H_{8,9},C_1H_{6,7}),s(C_{1,2},C_{3,4}),s(C_{2,5},C_{1,5})$
	1578.3	$sb(C_1H_{2,3},C_5H_{10,11,12})$
	1578.7	$sb(C_1H_{2,3}),sb(C_5H_{10,11,12})$
	1652.5	$ab(C_1H_{2,3}),abC_5H_{10,11,12}),b(C_2H_{11}),b(C_1H_{6,7})$
	1661.1	$ab(C_1H_{2,3}),ab(C_5H_{10,11,12}),b(C_2H_{11}),b(C_1H_{6,7})$
	1661.6	$ab(C_1H_{2,3}),ab(C_5H_{10,11,12})$
	1667.0	$ab(C_1H_{2,3}),ab(C_5H_{10,11,12}),b(C_2H_{11}),b(C_1H_{6,7})$
	1674.3	$ab(C_1H_{2,3},C_5H_{10,11,12}),b(C_2H_{11},C_1H_{6,7})$

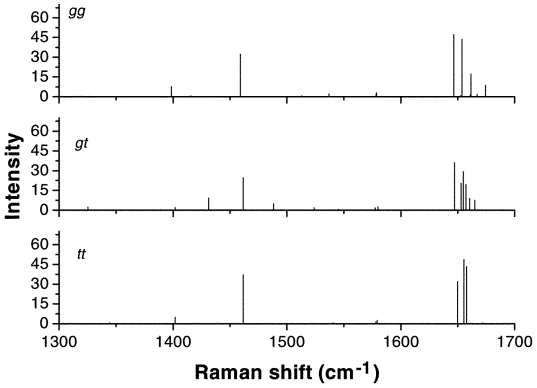

Fig. 9. Calculated Raman spectra of *n*-pentane in the region of 1300-1700 cm^{-1}.

vibrational modes, viz., methyl symmetric bending, methyl antisymmetric bending and methylene bending. The methyl antisymmetric bending mode was independent of the conformational change, e.g., *tt* at 1657.6 cm^{-1}, *gt* at 1657.2 cm^{-1} and *gg* at 1661.6 cm^{-1}. And the vibrational mode of in-phase methylene twisting mode had the same character. Hence, it was impossible to find some characteristic bands for each conformation from the higher intensities mentioned above. According to our calculations, some bands with weaker intensity were of great interest in the lower-frequency region. Among the three conformations, each conformation had its own bands, and thus the characteristic bands could be found. Hence, the bands at 1461.5 cm^{-1} and 1655.4 cm^{-1} belonged to *tt* conformation; 1431.2 cm^{-1}, 1653.0 cm^{-1} and 1660.5 cm^{-1} to *gt* conformation; 1459.1 cm^{-1} and 1674.3 cm^{-1} to *gg* conformation. Of course, these results would be confirmed by the experiments in the further work.

The calculated IR spectra (3150-3270 cm^{-1}) were shown in *Fig.* 10 and the assignments of main bands were listed in *Table* 8. In this region, the CH symmetric stretching mode and antisymmetric stretching mode were two main kinds of vibrational modes. Snyder[3] thought that the frequency and intensity for CH stretching tended to be independent of chain length. However the trend of frequency and intensity changes related to conformations was our major concern. Obviously, the bands of symmetric stretch-

Table 7. Calculated Raman frequency and description of 1300-1700 cm^{-1}

Conformation	Calculated frequency(cm^{-1})	Description
tt	1401.9	tw($C_1H_{2,3}$,C_2H_{12},$C_3H_{8,9}$,$C_4H_{11,12}$),tw($C_5H_{6,7}$)
	1461.5	tw(C_2H_{12},$C_3H_{6,7}$,$C_4H_{8,9}$)
	1649.7	b(C_2H_{12},$C_3H_{6,7}$,$C_4H_{8,9}$)
	1655.4	sb($C_1H_{2,3}$,$C_5H_{6,7,11,12}$),b(C_2H_{12},$C_4H_{8,9}$),b($C_3H_{6,7}$)
	1657.6	ab($C_1H_{2,3}$), ab($C_5H_{10,11,12}$)
gt	1401.8	tw(C_2H_{12},$C_4H_{8,9}$),tw($C_3H_{6,7}$)
	1431.2	tw($C_1H_{2,3}$,C_2H_{12},$C_3H_{6,7}$,$C_4H_{8,9}$)
	1461.6	tw(C_2H_{12},$C_3H_{6,7}$,$C_4H_{8,9}$)
	1488.4	w(C_2H_{12},$C_3H_{6,7}$,$C_4H_{8,9}$)
	1647.2	ab($C_1H_{2,3}$),b($C_3H_{6,7}$,$C_4H_{8,9}$)
	1653.0	ab($C_1H_{2,3}$,$C_5H_{6,7,11,12}$),b(C_2H_{12}),b($C_3H_{6,7}$)
	1654.8	b(C_2H_{12},$C_3H_{6,7}$),b($C_4H_{8,9}$),ab($C_5H_{10,11,12}$)
	1657.2	ab($C_5H_{6,7,11,12}$)
	1660.5	b($C_1H_{2,3}$),b(C_2H_{12},$C_3H_{6,7}$)
	1664.9	b(C_2H_{12},$C_3H_{6,7}$,$C_5H_{11,12}$),ab($C_1H_{2,3}$),b($C_4H_{8,9}$)
gg	1398.6	r($C_1H_{2,3}$,$C_5H_{10,11,12}$),tw($C_3H_{6,7}$)
	1459.1	tw(C_2H_{12},$C_3H_{6,7}$,$C_4H_{8,9}$)
	1646.5	ab($C_1H_{2,3}$,$C_5H_{6,7,11,12}$),b($C_3H_{6,7}$)
	1653.8	ab($C_1H_{2,3}$,$C_5H_{6,7,11,12}$),b(C_2H_{12},$C_3H_{6,7}$,$C_4H_{8,9}$)
	1661.6	ab($C_1H_{2,3}$),ab($C_5H_{6,7,11,12}$)
	1674.3	ab($C_1H_{2,3}$,$C_5H_{6,7,11,12}$),b(C_2H_{12},$C_4H_{8,9}$)

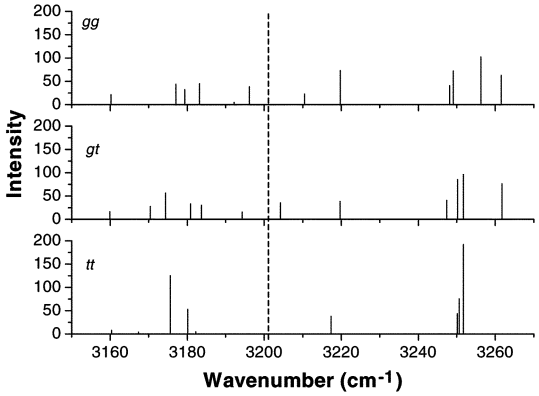

Fig. 10. Calculated IR spectra of *n*-pentane in the region of 3150-3270 cm^{-1}.

ing lay in the lower-frequency region, on the contrary, the bands of antisymmetric stretching lay in the higher-frequency region. Similar to other frequency regions, the number of bands with higher intensity of *tt* conformation was much less than that of *gt* and *gg* conformations. But the intensities in this region were much stronger than those in other regions. In the region of symmetric stretching, methyl symmetric stretching was an important vibrational mode, but a little wavenumber shift took place, *tt* at 3180.2 cm^{-1}, *gt* at 3180.9 cm^{-1} and *gg* at 3183.2 cm^{-1}. Besides, a band at 3175.6 cm^{-1} of *tt* conformation had so high intensity that it could be regarded as the characteristic band. Another characteristic band was at 3251.7 cm^{-1}. For *gt* and *gg* conformations, the characteristic bands of *gt* were at 3170.4 cm^{-1} and 3204.2 cm^{-1}, the characteristic bands of *gg* were at 3177.0 cm^{-1} and 3210.5 cm^{-1} in this region. In the higher-frequency region, the methyl antisymmetric stretching and methylene antisymmetric stretching were the main vibrational modes. For the out-of-

Table 8. Calculated IR frequency and description of 3150-3270 cm^{-1}

Conformation	Calculated frequency(cm^{-1})	Description
tt	3175.6	ss($C_1H_{3,5}$,$C_3H_{6,7}$,$C_4H_{10(11,12)}$),ss($C_2H_{4,5}$,$C_4H_{8,9}$)
	3180.2	ss($C_1H_{3,5}$),ss($C_3H_{10(11,12)}$)
	3217.3	as($C_1H_{3,5}$,$C_3H_{2,5}$,$C_2H_{8,9}$,$C_4H_{(1,0)}$),as($C_3H_{6,7}$)
	3250.1	as($C_1H_{3,5}$),as($C_3H_{10(11,12)}$)
	3250.6	as($C_1H_{3,5}$,$C_3H_{6(11,12)}$)
	3251.7	as($C_1H_{3,5}$,$C_3H_{2,5}$,$C_3H_{6,7}$,$C_4H_{8,9}$,$C_4H_{11,12}$)
gt	3170.4	ss($C_1H_{3,5}$,$C_3H_{6(11,12)}$),ss($C_2H_{4,5}$)
	3174.4	ss($C_1H_{3,5}$,$C_3H_{6(11,12)}$),ss($C_2H_{8,9}$)
	3180.9	ss($C_1H_{3,5}$),ss($C_3H_{10(11,12)}$)
	3183.7	ss($C_1H_{3,5}$),as($C_3H_{2,5}$,$C_2H_{8,9}$),as($C_3H_{6,7}$)
	3204.2	as($C_2H_{4,5}$),as($C_1H_{2,5}$,$C_4H_{8,9}$)
	3219.7	as($C_4H_{11,12}$),as($C_2H_{4,5}$,$C_3H_{6,7}$,$C_4H_{8,9}$)
	3247.4	as($C_1H_{3,5}$),as($C_3H_{10(11,12)}$)
	3250.2	as($C_4H_{9,12}$),as($C_1H_{1,2}$)
	3251.7	as($C_1H_{3,5}$,$C_3H_{6(11,12)}$),as($C_2H_{2,5}$,$C_3H_{6,7}$,$C_4H_{8,9}$)
	3261.8	as($C_1H_{3,5}$),as($C_3H_{10(11,12)}$)
gg	3177.0	ss($C_2H_{4,5}$),ss($C_2H_{8,9}$),as($C_3H_{6,7}$)
	3179.4	ss($C_1H_{3,5}$,$C_3H_{6(11,12)}$),ss($C_2H_{2,5}$,$C_3H_{6,7}$,$C_4H_{8,9}$)
	3183.2	ss($C_1H_{3,5}$),ss($C_3H_{10(11,12)}$)
	3196.2	as($C_2H_{4,5}$,$C_4H_{8,9}$),as($C_3H_{6,7}$)
	3210.5	as($C_1H_{3,5}$,$C_4H_{11,12}$),as($C_2H_{4,5}$,$C_4H_{8,9}$),ss($C_3H_{6,7}$)
	3219.8	ss($C_1H_{3,5}$),ss($C_3H_{10(11,12)}$),as($C_2H_{4,5}$,$C_3H_{6,7}$,$C_4H_{8,9}$)
	3248.1	as($C_1H_{3,5}$,$C_4H_{11,12}$)
	3249.1	as($C_1H_{3,5}$,$C_4H_{10,12}$),as($C_2H_{4,5}$,$C_3H_{6,7}$,$C_2H_{8,9}$)
	3256.3	as($C_1H_{3,5}$),as($C_3H_{10(11,12)}$)
	3261.8	as($C_1H_{3,5}$,$C_4H_{6(11,12)}$),as($C_2H_{2,5}$,$C_4H_{8,9}$)

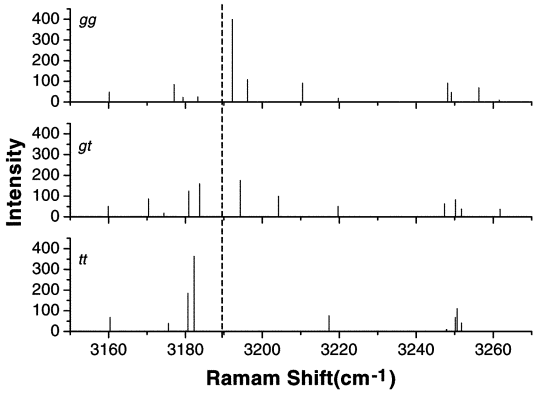

Fig. 11. Calculated Raman spectra of *n*-pentane in the region of 3150-3270 cm^{-1}.

phase methyl antisymmetric stretching, its frequency had a biggish shift, *tt* at 3250.1 cm^{-1}, *gt* at 3261.8 cm^{-1} and *gg* at 3256.3 cm^{-1}. In the spectra of *tt* conformation, the band with the strongest intensity was in-phase C-H antisymmetric stretching, at 3251.7 cm^{-1}, hence it could be considered as a characteristic band. In addition, one of the most intriguing frequencies was near 3200 cm^{-1}. It formed the division between the symmetric stretching and the antisymmetric stretching (dashed in *Fig.* 10).

The calculated Raman spectra (3150-3270 cm^{-1}) were shown in *Fig.* 11 and the assignments of main bands were listed in *Table* 9. Different from the calculated IR spectra, the bands with higher intensities lay in the lower-frequency region. But because of the coupling of each vibrational mode, it was very difficult to find the same mode. Although some bands with the approximate frequency, their vibrational modes were different, e.g., the band at 3160.4 cm^{-1} of *tt* conformation, the band at 3159.9 cm^{-1} of *gt*

Table 9. Calculated Raman frequency and description of 3150-3270 cm^{-1}

Conformation	Calculated frequency(cm^{-1})	Description
tt	3160.3	$ss(C_2H_{4,5},C_3H_{6,7}\text{-}C_4H_{8,9}),ss(C_1H_{1,2,3},C_5H_{10,11,12})$
	3175.6	$ss(C_1H_{1,2,3},C_3H_{6,7}\text{-}C_5H_{\text{-}10,11,12}),ss(C_2H_{4,5}\text{-}C_4H_{8,9})$
	3180.7	$as(C_2H_{4,5},C_4H_{8,9}),as(C_3H_{6,7})$
	3182.2	$ss(C_1H_{1,2,3},C_2H_{4,5},C_3H_{6,7}\text{-}C_4H_{8,9}\text{-}C_5H_{10,11,12})$
	3217.3	$as(C_1H_{2,3},C_2H_{4,5}\text{-}C_4H_{8,9}\text{-}C_5H_{11,12}),as(C_3H_{6,7})$
	3250.1	$as(C_1H_{1,2,3}),as(C_5H_{\text{-}10,11,12})$
	3250.6	$as(C_1H_{1,2,3},C_5H_{10,11,12})$
	3251.7	$as(C_1H_{2,3},C_2H_{4,5}\text{-}C_3H_{6,7}\text{-}C_4H_{8,9}\text{-}C_5H_{11,12})$
gt	3159.9	$ss(C_2H_{4,5}),ss(C_3H_{6,7}\text{-}C_4H_{8,9})$
	3170.4	$ss(C_1H_{1,2,3},C_5H_{10,11,12}),ss(C_2H_{4,5})$
	3180.9	$ss(C_1H_{1,2,3}),ss(C_5H_{\text{-}10,11,12})$
	3183.7	$ss(C_1H_{1,2,3}),as(C_2H_{4,5}\text{-}C_4H_{8,9}),as(C_3H_{6,7})$
	3194.3	$ss(C_1H_{1,2,3},C_2H_{4,5}),as(C_3H_{6,7}),as(C_4H_{8,9})$
	3204.2	$as(C_2H_{4,5}),as(C_1H_{2,3}\text{-}C_4H_{8,9})$
	3219.7	$as(C_5H_{11,12}),as(C_2H_{4,5}\text{-}C_3H_{6,7}\text{-}C_4H_{8,9})$
	3247.4	$as(C_1H_{1,2}),as(C_5H_{\text{-}10,11,12})$
	3250.2	$as(C_5H_{10,12}),as(C_1H_{1,2})$
	3251.7	$as(C_1H_{1,2,3},C_5H_{10,11,12}),as(C_2H_{4,5}\text{-}C_3H_{6,7}\text{-}C_4H_{8,9})$
	3261.8	$as(C_1H_{1,2,3}),as(C_5H_{\text{-}10,11,12})$
gg	3160.2	$ss(C_3H_{6,7})$
	3177.0	$ss(C_2H_{4,5}),ss(C_4H_{8,9}),as(C_3H_{6,7})$
	3192.2	$ss(C_1H_{1,2,3},C_5H_{10,11,12}),ss(C_2H_{4,5}\text{-}C_3H_{6,7}\text{-}C_4H_{8,9})$
	3196.2	$as(C_2H_{4,5},C_4H_{8,9}),as(C_3H_{6,7})$
	3210.5	$as(C_1H_{2,3},C_5H_{11,12}),as(C_2H_{4,5},C_4H_{8,9}),ss(C_3H_{6,7})$
	3248.1	$as(C_1H_{1,2},C_5H_{11,12})$
	3249.1	$as(C_1H_{1,2},C_5H_{10,12}),as(C_2H_{4,5},C_3H_{6,7},C_4H_{8,9})$
	3256.3	$as(C_1H_{1,2,3}),as(C_5H_{\text{-}10,11,12})$

conformation and the band at 3160.2 cm^{-1} of *gg* conformation. On the other hand, the division between symmetric stretching and antisymmetric stretching shifted to near 3190 cm^{-1} (dashed in *Fig.* 11), but there appeared an exception at about 3180 cm^{-1}, viz. the frequency of antisymmetric stretching was smaller than that of symmetric stretching. In the higher-frequency region, the methyl antisymmetric stretching mode was the main vibrational mode. The change trend of this mode was the same as that in IR spectra. *tt* at 3250.1 cm^{-1}, *gt* at 3261.8 cm^{-1} and *gg* at 3256.3 cm^{-1}. In the spectra of *gg* conformation, the characteristic bands were at 3170.4 cm^{-1} and 3204.2 cm^{-1}. For *gt* conformation, the characteristic bands were at 3177.0 cm^{-1} and 3210.5 cm^{-1}. For *tt* conformation, the characteristic bands were at 3182.2 cm^{-1} and 3217.3 cm^{-1}.

CONCLUSIONS

In this work, we investigated the overall IR and Raman spectra of *n*-pentane by *ab initio* calculations. The Hartree-Fock (HF) method and the 6-31G basis set provided a good description of normal mode frequencies and intensities of three stable conformations of *n*-pentane. Analyzing the IR and Raman spectra respectively, the frequency region was divided into four parts: 0-600 cm^{-1}, 700-1300 cm^{-1}, 1300-1700 cm^{-1} and 3150-3270 cm^{-1}. Each region was discussed in detail and some characteristic bands with corresponding vibrational modes were reassigned. For different conformations, there were some different characteristic bands. Some of them could not be obtained by experiments, especially for some broad bands. But in the present work, this question could be avoided. Hence, it was possible to find the overall spectra information including IR and Raman of each conformation. The bands in the IR spectra were found to be associated with specific conformations: 196.4 cm^{-1}, 803.4 cm^{-1}, 995.4 cm^{-1}, 1172.7 cm^{-1}, 1656.9 cm^{-1}, 1672.0 cm^{-1}, 3175.6 cm^{-1} and 3251.7 cm^{-1} for *tt* conformation; 511.7 cm^{-1}, 844.2 cm^{-1}, 915.8 cm^{-1}, 1174.1 cm^{-1}, 1523.8 cm^{-1}, 1660.5 cm^{-1}, 3170.4 cm^{-1} and 3204.2 cm^{-1} for *gt* conformation; 517.9 cm^{-1}, 807.2 cm^{-1}, 922.6 cm^{-1}, 1652.5 cm^{-1}, 1667.0 cm^{-1}, 1674.3 cm^{-1}, 3177.0 cm^{-1} and 3210.5 cm^{-1} for *gg* conformation. In the Raman spectra, the bands were as follows: 428.6 cm^{-1}, 951.4 cm^{-1}, 1132.8 cm^{-1}, 1278.0 cm^{-1}, 1461.5 cm^{-1}, 1655.4 cm^{-1}, 3182.2 cm^{-1} and 3217.3 cm^{-1} for *tt* conformation; 511.7 cm^{-1}, 844.2 cm^{-1}, 915.8 cm^{-1}, 1431.2 cm^{-1}, 1653.0 cm^{-1}, 1660.5 cm^{-1}, 3170.4 cm^{-1} and 3204.2 cm^{-1} for *gt* conformation; 517.9 cm^{-1}, 922.6 cm^{-1}, 1083.8 cm^{-1}, 1126.2 cm^{-1}, 1459.1 cm^{-1}, 1674.3 cm^{-1}, 3177.0 cm^{-1} and 3210.5 cm^{-1} for *gg* conformation. Likewise, the trend of frequency changes with the same vibrational mode was discussed. According to the trend discussed above, we could predict the change of conformation for experiments. At the same time, we also wanted to demonstrate the applicability and usefulness of *ab initio* calculated spectra for elucidating the spectra of long chain *n*-alkanes and their conformations in the future work.

Acknowledgements. This work is supported by the NSFC (20073004, 20473012), Fundamental Foundation of BIT and the Trans-Century Training Program Foundation for the Talents by the Ministry of Education of China are also gratefully acknowledged.

REFERENCES

1. Snyder, R. G.; Schachtschneider, J. H. *Spectrochim. Acta.*, **1963**, *19*, 85.
2. Schachtschneider, J. H.; Snyder, R. G. *Spectrochim. Acta.*, **1963**, *19*, 117.
3. Snyder, R. G. *J. Chem. Phys.*, **1967**, *47*, 1316.
4. Aljibury, A. L.; Snyder, R. G.; Strauss, H. L.; Raghavachari, K. *J. Chem. Phys.*, **1986**, *84*, 6872.
5. Raghavachari, K. *J. Chem. Phys.*, **1984**, *81*, 1383.
6. Murphy, W. F.; Fernandez-Sanchez, J. M.; Raghavachari, K. *J. Phys. Chem.*, **1991**, *95*, 1124.
7. Durig, J. R.; Wang, A.; Beshir, W.; Little, T. S. *J. Raman. Spectroscop.*, **1991**, *22*, 683.
8. DeFrees, D. J.; Levi, B. A.; Pollack, S. K.; Hehre, W. J.; Binkley, J. S.; Pople, J. A. *J. Am. Chem. Soc.*, **1979**, *101*, 4085.
9. Ditchfield, R.; Heher, W. J.; Pople, J. A. *J. Chem. Phys.*, **1971**, *54*, 724.
10. Guogh, K. M.; Murphy, W. F. *J. Chem. Phys.*, **1987**, *87*.

3332.
11. Radom, L.; Lathan, W. A.; Hehre, W. J.; Pople, J. A. *J. Am. Chem. Soc.*, **1973**, *95*, 693.
12. Peterson, M. R.; Csizmadia, I. G. *J. Am. Chem. Soc.*, **1978**, *100*, 6911.
13. Scheiner, S. *J. Am. Chem. Soc.*, **1980**, *102*, 3723.
14. Darsey, J. A.; Rao, B. K. *Macromolecules.*, **1981**, *14*, 1575.
15. Van-Catledge, F. A.; Allinger, N. L. *J. Am. Chem. Soc.*, **1982**, *104*, 6272.
16. Wiberg, K. B.; Murcko, M. A. *J. Am. Chem. Soc.*, **1988**, *110*, 8029.
17. Scarsdale, J. N.; Van Alsenoy, C.; Schafer, L. *J. Mol. Struc (THEOCHEM).*, **1982**, *86*, 277.
18. Schafer, L.; Siam, K.; Ewbank, J.; Osawa, E. *J. Mol. Struc (THEOCHEM).*, **1986**, *139*, 125.
19. Mirkin, N. G.; Krimm, S. *J. Phys. Chem.*, **1993**, *97*, 13887.
20. Snyder, R. G.; Kim, Y. *J. Phys. Chem.*, **1991**, *95*, 602.
21. Zeigler, R. C.; Maciel, G. E. *J. Am. Chem. Soc.*, **1991**, *113*, 6349.
22. Zeigler, R.C.; Maciel, G. E. *J. Phys. Chem.*, **1991**, *95*, 7345.
23. Pursch, M. S.; Handel, S. H. *Anal. Chem.*, **1996**, *68*, 386.
24. Ohtake, T.; Mino, N.; Ogawa, K. *Langmuir*, **1992**, *8*, 2081.
25. Tripp, C. P.; Hair, M. L. *Langmuir*, **1992**, *8*, 1120.
26. Shashikala, S.; Jurgen, W.; Klaus, A. *J. Phys. Chem. B.*, **2002**, *106*, 878.
27. Ho, M.; Cai, M.; Pemberton, J. E. *Anal. Chem.*, **1997**, *69*, 2613.
28. Frisch, M. J.; Trucks, G. W.; Schlegel, H. B.; Scuseria, G. E.; Robb, M. A.; Cheeseman, J. R. *GAUSSIAN 98, Revision A. 9*. Gaussian, Inc., Pittsburgh, PA, **1998**.
29. Mirkin, N. G.; Krimm, S. *J. Mol. Struc.*, **2000**, *550-551*, 67.
30. Nelligan, W. B.; LePoire, D. J. *J. Chem. Phys.*, **1987**, *87*, 2447.
31. Tomonaga, A.; Shimanouchi, T. *Bull. Chem. Soc. Jpn.*, **1968**, *41*, 1446.